THE JOURNAL OF PHYSICAL CHEMISTRY C

Article

pubs.acs.org/JPCC

Poisoning of Hydrogen Recombination on Silica Due to Water Adsorption

Kyle K. Mackay, Harley T. Johnson,* and Jonathan B. Freund

Department of Mechanical Science and Engineering, University of Illinois at Urbana—Champaign, Urbana, Illinois 61801, United States

ABSTRACT: The role of water adsorption in poisoning hydrogen recombination on silica is studied using a two-layer Langmuir isotherm model. In the model, hydrogen atoms adsorb directly on the silica surface, while water molecules physisorb above the surface, blocking gas atoms from reaching or reacting on the surface. Model parameters such as heat of adsorption and activation energy are informed using experimental values and data from atomic-scale simulations. Using this model for a gas-phase radical concentration of 10^{16} cm^{-3} (representative of a room-temperature gas at 1 Torr), the addition of water vapor is predicted to lower the room-temperature recombination coefficient of hydrogen (γ_H) from 3×10^{-3} to 2×10^{-4}, consistent with experimental data. In general, surface reaction rates are reduced significantly for temperatures below 400 K. An analytical model is used to estimate the effect of reactive walls on radical concentration in a silica tube used in hydrogen plasma experiments. In the model, radical concentration is held constant at one end of the tube, and radical species diffuse down its length and to the walls of the tube, where they are destroyed by recombination reactions. The poisoning effect of water on surface reactions greatly enhances radical concentration in the tube, increasing the fraction of unreacted radicals 30 cm from the inlet by nearly 2 orders of magnitude. Both the reduction of the room-temperature recombination coefficient and the increased concentration of atomic hydrogen in the silica tube are in quantitative agreement with experimental findings.

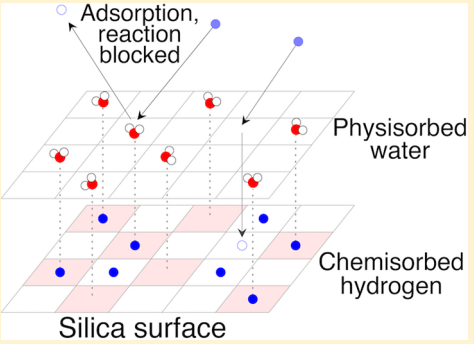

1. INTRODUCTION

The hydrophilic/hydrophobic character of silica surfaces has attracted much attention, making it a popular candidate material for studies of surface wettability.[1−9] The general hydrophilicity is attributed to the presence of silanol (Si−O−H) groups on exposed surfaces. At high temperatures, these groups are progressively removed through mutual condensation. This process produces a water molecule and a siloxane bridge on the surface (Si−O−Si), resulting in a hydrophobic quartz surface.[10] In addition to controlling surface wettability, these silanol groups can serve as active sites for adsorption and heterogeneous recombination of reactive species. In particular, the adsorption of hydrogen atoms on these sites is believed to be an indispensible step in the heterogeneous recombination of hydrogen on silica.[11−13]

Such surface reactions are thought to be important in a range of applications. Recombination of hydrogen on glass is thought in cases to contaminate vacuum experiments, obscuring the phenomena being studied and destroying radicals.[14−16] Knowledge of recombination rates under various conditions and in different gas mixtures allows for such effects to be predicted and thus accounted for or minimized in the design and operation of hydrogen plasma and combustion devices.

It is known from experiments that the addition of water vapor to the feed gas (or adding oxygen, which reacts to form water in the discharge) can greatly boost radical production in a plasma,[17,18] which has been attributed to two possible mechanisms:

1. the generation of OH radicals that can react with H_2 to form a H radical and a water molecule (opening a new pathway for H_2 dissociation) and
2. the "poisoning" (slowing) of heterogeneous hydrogen recombination on the inner wall of the silica tube downstream of the plasma.

Each of these effects has been observed, but their relative contribution to increased H production in particular applications is unclear.[19,20]

The affinity of water molecules for silica surfaces has been investigated extensively, in wettability studies and in measurement of the large heat of adsorption of water on hydroxylated silica.[21,22] However, models for the poisoning effect of water on hydrogen recombination (and proper surface chemistry models for silica in general) are still lacking. The goal of this study is to develop a surface chemistry model to describe the poisoning of hydrogen recombination by water adsorbed on silica.

Isotherm models of the silica surface are introduced in Sections 2.1 and 2.2. The surface reaction mechanisms are added in Section 2.3. Calculation of surface coverages and recombination coefficients are outlined in Sections 2.4 and 2.5, respectively. The resulting effect of water on hydrogen recombination rates is quantified in Section 3.1. The effect of

Received: May 15, 2017
Revised: June 26, 2017
Published: July 10, 2017

DOI: 10.1021/acs.jpcc.7b04675
J. Phys. Chem. C 2017, 121, 16366−16372

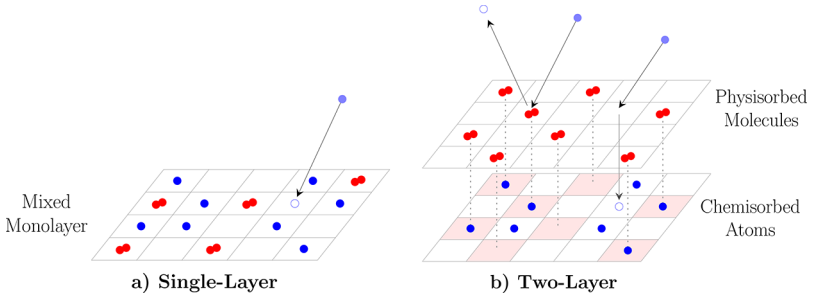

Figure 1. Schematics of the Langmuir isotherm models used in this study. In the single-layer model (a), water and hydrogen atoms adsorb in the same monolayer. In the two-layer model (b), physisorbed molecules (red) block incoming radicals (blue) from adsorbing or reacting on the chemisorption layer below. Blocked chemisorption sites are represented by pink squares.

this poisoning on a model experimental setup is examined in Section 3.2, and the results of this model are compared with reported experiments in Section 3.3, which is followed by a summary of the principal conclusions.

2. THEORY

2.1. Two-Layer Langmuir Isotherm. A schematic of the two-layer isotherm model is shown in Figure 1. We use a two-layer Langmuir isotherm composed of a discrete set of adsorption sites that can accommodate only a single molecule at a time. The bottom layer represents chemisorbed species tightly bound to the surface, and the top layer represents relatively weakly bound physisorbed species. Similar models have been used to reproduce the non-Arrhenius recombination rates on silica surfaces seen in experimental and computational studies.[13,23] In our model, the adsorbed water molecules reside in the physisorption top layer and block radical species from reaching chemisorption sites on the surface in the bottom layer. This physisorbed shield layer of water molecules thus hinders adsorption and the Eley–Rideal mechanism, poisoning surface reactions.

In the two-layer model, the surface is initially free of adsorbed species. Empty chemisorption sites represent strained siloxane bridges that bind atomic hydrogen during the chemisorption process to form silanol groups on the surface. The region above each silanol group provides a physisorption site for water, so chemisorption and physisorption sites in this model are collocated with the same site density.

There are three distinct types of silanol configurations that manifest themselves on silica surfaces (isolated, viscinal, and geminal) with minor variations in heat of formation and the heat of adsorption of water on the defect. In both isotherm models, all silanol groups are given properties corresponding to the ensemble average of silanol groups measured in experiments and electronic-scale calculations.[24,25]

Because water has a significantly higher heat of physisorption relative to hydrogen (13 vs 2–3 kcal/mol), exchange of hydrogen between the layers is ignored, as the physisorption layer will be almost exclusively populated by water for mixtures containing water vapor.

2.2. Single-Layer Langmuir Isotherm. Results obtained with our two-layer model are contrasted with a single-layer Langmuir isotherm model. In this model, hydrogen atoms and water molecules adsorb in a common monolayer and compete for the same adsorption sites on the surface. In the single-layer model, the species with higher heat of adsorption dominate and cover a majority of the surface. Because atomic hydrogen has a higher heat of adsorption than water, we would expect water to have a diminished poisoning effect in the single-layer model.

2.3. Surface Processes. For both isotherm models, we include four types of reactions. Both inert and reactive species can adsorb and desorb from their respective layers. In addition, radical species in the chemisorption layer may also participate in the Eley–Rideal and Langmuir–Hinshelwood recombination reactions. In the two-layer model, quantities with a subscript C apply to processes in the chemisorption layer while those with a subscript P apply to processes in the physisorbed shield layer.

2.3.1. Adsorption and Sticking Probability. Adsorption is represented by

$$\mathrm{H(g)} \xrightarrow{R^{\mathrm{A}}} \mathrm{H(s)}$$

For an ideal gas, the rate at which gas particles impact the surface is

$$k^{\mathrm{in}} = n_{\mathrm{g}}\left(\frac{k_{\mathrm{B}}T}{2\pi m}\right)^{1/2} \tag{1}$$

where k_{B} is the Boltzmann constant and n_{g}, T, and m are the number density, temperature, and molecular weight of the gas-phase species. Not all incident atoms adsorb to the surface—only those that reach empty adsorption sites can form bonds with the surface, so the rate of adsorption is

$$R^{\mathrm{A}} = s(T)(1-\theta)k^{\mathrm{in}} \tag{2}$$

where θ is the fraction of occupied adsorption sites and $s(T)$ is the sticking probability for atoms that reach empty adsorption sites. The adsorption of water molecules is hindered only by the availability of top-layer physisorption sites, while chemisorption of radicals is hindered both by the availability of bottom-layer chemisorption sites and by water molecules in the top physisorption layer; so the corresponding net reaction rates are

$$R_{\mathrm{P}}^{\mathrm{A}} = s(T)(1-\theta_{\mathrm{p}})k^{\mathrm{in}} \tag{3}$$

$$R_{\mathrm{C}}^{\mathrm{A}} = s(T)(1-\theta_{\mathrm{C}})(1-\theta_{\mathrm{p}})k^{\mathrm{in}} \tag{4}$$

To include the effect of temperature, we employ the simple Baule–Weinberg–Merrill model,[26] represented in Figure 2. It predicts that incident atoms will be trapped if the component of kinetic energy normal to the surface is below the threshold

$$E_{\mathrm{crit}} = \frac{4\left(\frac{m}{m_{\mathrm{s}}}\right)}{\left(1-\frac{m}{m_{\mathrm{s}}}\right)^2}(Q_{\mathrm{p}} - 0.5k_{\mathrm{B}}T) \tag{5}$$

DOI: 10.1021/acs.jpcc.7b04675
J. Phys. Chem. C 2017, 121, 16366–16372

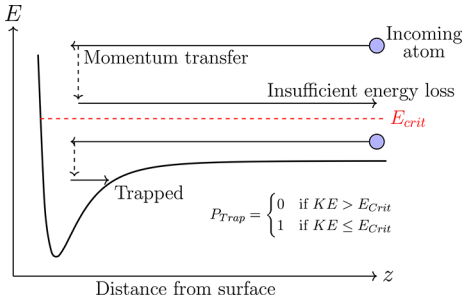

Figure 2. Depiction of the Baule–Weinberg–Merrill trapping model used to determine sticking probability in our isotherm model. The potential well near the surface is represented with a thick black line and gas atoms with blue circles.

Otherwise the atom scatters. In eq 5, the potential energy well depth is set as the heat of physisorption Q_P; T is the surface temperature; m is the mass of a gas atom; and m_s is the mass of a surface atom. We assume equilibrium conditions in the gas and calculate the average trapping probability for gas atoms by averaging over the Maxwell–Boltzmann energy distribution, so that

$$s(T) = \frac{1}{\sqrt{2\pi m k_B T}} \int P_{trap}(E_z) \exp\left[-\frac{E_z}{2\pi m k_B T}\right] dE_z \quad (6)$$

where E_z is the energy associated with the normal velocity, which needs to be absorbed by the surface. For the Baule–Weinberg–Merrill model, $P_{trap}(E_z) = 0$ for $E_z > E_{crit}$ and $P_{trap}(E_z) = 1$ for $E_z < E_{crit}$, so

$$s(T) = \mathrm{erf}\left(\sqrt{\frac{E_{crit}}{k_B T}}\right) \quad (7)$$

Since the quartz surface is composed of multiple elements (Si and O), we calculate $s(T)$ using E_{crit} determined by oxygen atom mass ($s_O(T)$) and silicon atom mass ($s_{Si}(T)$) and set the total sticking probability to a reference level of

$$s_{tot}(T) = \frac{1}{3} s_{Si}(T) + \frac{2}{3} s_O(T)$$

based on the stoichiometry of quartz. It should be noted that silica generally prefers oxygen atoms at the surface, but our results are not sensitive to the weights we assign to the elements here.

2.3.2. Eley–Rideal Recombination. The first recombination mechanism considered is the Eley–Rideal pathway, where a gas-phase hydrogen atom directly impinges on an adsorbed hydrogen atom and recombines or

$$H(g) + H(s) \xrightarrow{R^{ER}} H_2(g)$$

The probability of an incident atom recombining with an adsorbed atom on a fully covered surface is

$$p_{ER} = 2gN_0\sigma_0 \exp\left[-\frac{E_{ER}}{k_B T}\right] \quad (8)$$

where $g = 0.25$ is a statistical factor to account for the electronic degeneracies of the H atom and the H_2 molecule;[12,27] N_0 is the density of adsorption sites per unit area; σ_0 is the collisional cross-section of an adsorbed atom; and E_{ER} is the activation energy of ER recombination. Cross section σ_0 is approximated using the bond length of H_2

$$\sigma_0 = \pi r_{H_2}^2 = 1.72 \times 10^{-16}\ \mathrm{cm}^2$$

The overall rate of the ER reaction is

$$R_C^{ER} = (1 - \theta_P)\theta_C k_C^{ER} = (1 - \theta_P)\theta_C k^{in} p_{ER} \quad (9)$$

where the prefactor of $(1 - \theta_P)$ accounts for incident atoms blocked by the shield layer. From Hirschfelder's semiempirical model based on hydrogen reaction rates, we take the activation energy for ER hydrogen recombination to be

$$E_{ER} = 0.055 Q_C$$

where Q_C is the heat of chemisorption.[12,13,28]

2.3.3. Langmuir–Hinshelwood Recombination. At higher temperatures, adsorbed atoms are more mobile, and a second recombination pathway opens

$$H(s) + H(s) \xrightarrow{R^{LH}} H_2(g)$$

This reaction is second order with surface coverage, so

$$R_C^{LH} = \theta_C^2 k_C^{LH} = \theta_C^2 C_{LH} \exp\left[-\frac{E_{LH}}{k_B T}\right] \quad (10)$$

with a pre-exponential factor C_{LH} and activation energy E_{LH}. This reaction only occurs between atoms already adsorbed in the chemisorption layer, so there is no effect of the shield layer. This reaction is expected to be dominant in the high-temperature regime, presumably after most of the molecules physisorbed in the shield layer have desorbed from the surface. Based on atomic-scale simulations of hydrogen recombination,[23] we set the activation energy for LH hydrogen recombination to 21.96 kcal/mol.

2.3.4. Thermal Desorption. We also include thermal desorption, which becomes important at even higher temperatures

$$H(s) \xrightarrow{k^D} H(g)$$

with overall reaction rates

$$R_C^D = \theta_C k_C^D = \theta_C C_C^D \exp\left[-\frac{Q_{C,H}}{k_B T}\right] \quad (11)$$

$$R_P^D = \theta_P k_P^D = \theta_P C_P^D \exp\left[-\frac{Q_{P,H2O}}{k_B T}\right] \quad (12)$$

with pre-exponential factors C^D and activation energy determined by the heats of chemisorption Q_C and physisorption Q_P. Because chemidesorption is dominant only at high temperatures, any effects of the shield layer on this reaction are neglected because the more weakly bound physisorbed molecules will have almost completely desorbed.

Values used for the thermal desorption pre-exponential factors are likewise based on atomic-scale simulations of hydrogen–silica interactions[23] and semiequilibrium theory[12]

$$C_C^D = 3.4 \times 10^{26}\ 1/\mathrm{cm}^2\ \mathrm{s}\ \text{for chemisorbed hydrogen}$$

$$C_P^D = 1.1 \times 10^{27}\ 1/\mathrm{cm}^2\ \mathrm{s}\ \text{for physisorbed water}$$

2.4. Calculated Surface Coverages. In the two-layer model, it is necessary to first calculate the steady-state coverage of water in the physisorption layer. Equilibrium $R_P^A = R_P^D$ yields

DOI: 10.1021/acs.jpcc.7b04675
J. Phys. Chem. C 2017, 121, 16366–16372

$$(1-\theta_P)k_P^A = \theta_P k_P^D \rightarrow \theta_P = \frac{k_P^A}{k_P^A + k_P^D} \quad (13)$$

The coverage of the physisorption layer is then used in the rates of chemisorption and Eley–Rideal recombination to find steady-state chemisorption coverage by using the zero-flux condition $R_C^A = R_C^D + 2R_C^{LH} + R_C^{ER}$ or

$$\underbrace{s(T)(1-\theta_C)(1-\theta_P)k^{in}}_{\text{H onto surface}} = \underbrace{(1-\theta_P)\theta_C k_C^{ER} + 2\theta_C^2 k_C^{LH} + \theta_C k_C^D}_{\text{H \& } H_2 \text{ off of surface}} \quad (14)$$

to solve for θ_C.

2.5. Recombination Coefficient. Finally, we define the overall surface reactivity with recombination coefficient γ. This parameter represents the probability that an incident radical (an H atom in this case) will react and leave the surface as part of a stable molecule (H_2). Given the surface coverages and reaction rates

$$\gamma = \frac{(1-\theta_P)\theta_C k_C^{ER} + 2\theta_C^2 k_C^{LH}}{k_C^{in}} \quad (15)$$

3. RESULTS AND DISCUSSION

3.1. Recombination Coefficient. The procedure outlined in Section 2 was used to calculate the recombination coefficient for hydrogen atoms across a wide temperature range with and without water vapor. The conditions were selected to represent corresponding experimental conditions (1 Torr and 0.1 water mixture ratio).[17] The same conditions are tested again with the water concentration halved (a mixture ratio of 0.05) to test the sensitivity of the poisoning effect to water concentration. Relevant physical and model parameters are listed in Table 1. We assume the surface is in thermal equilibrium with the gas.

Table 1. Values Used in the Isotherm Models

parameter	value
N_0	9.30×10^{14} cm^{-2}[23]
n_H	3.22×10^{16} cm^{-3}
n_{H2O} (10%)	0.35×10^{16} cm^{-3}
n_{H2O} (5%)	0.175×10^{16} cm^{-3}
$Q_{P,H}$	2.18 kcal/mol[23]
$Q_{C,H}$	46.06 kcal/mol[23]
$Q_{P,H2O}$	13.20 kcal/mol[24,25]

Temperature dependence of recombination on the poisoned and unpoisoned silica surface is shown in Figure 3. With water vapor, recombination rates drop significantly in the two-layer model. The room-temperature recombination coefficient drops from its unpoisoned value of $\gamma(300\text{ K}) \approx 3 \times 10^{-3}$ to $\gamma(300\text{ K}) \approx 1 \times 10^{-4}$. The reduction in recombination activity is even more severe as temperature is reduced, and water condensation blocks more active sites on the surface. Above 450 K, most water has desorbed from the surface, with the result that poisoning is negligible at high temperatures. With water concentration reduced by a factor of 2, the poisoning effect on hydrogen recombination is essentially unchanged. For all temperatures, the difference between the recombination coefficient for the water-containing mixtures is less than 10%.

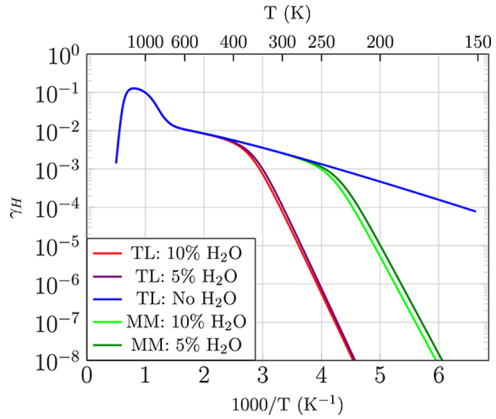

Figure 3. Recombination coefficient for H radicals in a pure H–H_2 gas (blue line) and with water vapor added to the mixture (red and violet lines), as calculated by the two-layer (TL) model. Results for a mixed monolayer (MM) of water and hydrogen radicals are shown in light and dark green.

Because hydrogen radicals have a higher heat of adsorption than water on the silica surface, atomic hydrogen is preferentially adsorbed in the single-layer model. As a result, the poisoning effect of water is diminished—when water and hydrogen adsorb in a mixed monolayer, hydrogen recombination rates are unaffected at temperatures above 250 K. For lower temperatures, the single-layer model predicts a drop-off similar to the two-layer model. While the effect of halving water concentration is still somewhat small in the mixed monolayer model, the sensitivity of poisoning to water concentration is greater than in the two-layer model.

Figure 4 shows the sensitivity of each model to the surface binding energy of water and hydrogen. The poisoning effect in

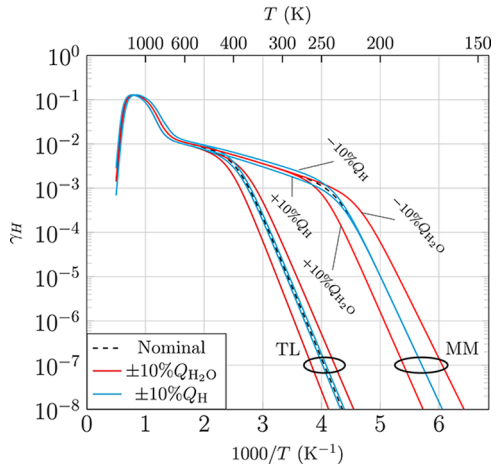

Figure 4. Sensitivity study of the variation in recombination coefficient to physisorption bond energy of water and the chemisorption bond energy of hydrogen in the two-layer (TL) and mixed monolayer (MM) models.

the mixed monolayer model is generally more sensitive to binding energies than the two-layer model. The recombination coefficient predicted by each model is also more sensitive to the binding energy of water than hydrogen, and decreasing the binding energy of either species to the surface results in a higher recombination coefficient. Decreasing the heat of adsorption of water reduces the amount of water on the

DOI: 10.1021/acs.jpcc.7b04675
J. Phys. Chem. C 2017, 121, 16366–16372

surface at equilibrium, reducing the poisoning effect on hydrogen recombination. Decreasing the heat of chemisorption of hydrogen on the surface will reduce the equilibrium surface coverage of hydrogen; however, the lower binding energy also means a lower activation energy for heterogeneous recombination. This results in a net increase of heterogeneous recombination rates when the heat of chemisorption of hydrogen is decreased.

3.2. Diffusive Transport in a Reactive Tube. In an apparatus commonly used to study heterogeneous reaction rates, radical species are generated by a plasma at one end of a tube with reactive walls (Figure 5). Reactive molecules diffuse

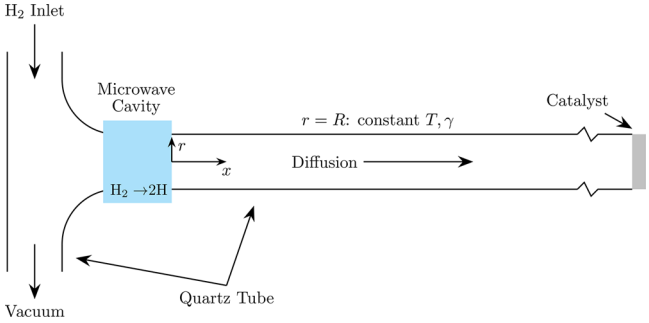

Figure 5. Schematic of an experimental apparatus frequently used to quantify recombination rates on silica. Hydrogen radicals are generated in a microwave plasma and diffuse down a silica tube, recombining on the inner walls. Any remaining radicals that reach the end of the tube are destroyed by a catalyst.[11,17]

down the tube and are consumed by reactions on the surface. The recombination coefficient of these reactive species is determined by measuring the decay of radical concentration along the axis of the tube.

An analytical solution for radical concentration has been obtained for this system, with the assumptions that (1) radical concentration is uniform at the inlet, (2) convective transport is negligible, and (3) diffusivity and recombination coefficient are uniform down the length of the tube.[29] The steady-state radical concentration is given by

$$n(r, x) = \sum_{i=1}^{\infty} A_i J_0(\xi_i r)\exp(-\xi_i x) \tag{16}$$

where

$$A_i = \frac{2n_0}{R\xi_i(1 + \delta^2 R^2 \xi_i^2) J_1(\xi_i R)} \tag{17}$$

and ξ_i are the positive roots of the equation

$$J_0(\xi R) = \delta R \xi J_1(\xi R) \tag{18}$$

Here, R is the radius of the tube; J_0 and J_1 are Bessel functions; n_0 is the radical concentration at the inlet; and δ is the similarity parameter, given by

$$\delta = \frac{4D}{\gamma c R}\frac{(2-\gamma)}{2} \tag{19}$$

where D is the diffusivity of radical species and c is the mean atomic velocity in any one dimension, given by

$$c = \sqrt{\frac{2k_B T}{\pi m}} \tag{20}$$

This analytic solution was used, along with our poisoned and unpoisoned recombination coefficients at room temperature, to model the corresponding experimental setup.[17] The diffusivity of hydrogen atoms in the H_2 gas was calculated using the mean free path estimate of the binary diffusion coefficient

$$D_{H-H_2} = \frac{8}{3p(d_H + d_{H_2})^2}\sqrt{\frac{k_B^3 T^3}{\pi^3}}\sqrt{\frac{1}{2m_H} + \frac{1}{2m_{H_2}}} \tag{21}$$

where m is atomic mass; d is molecular diameter; and p is pressure of the mixture.[30] Experimental and model parameters are listed in Table 2. L represents the x-position where radical

Table 2. Values Used in an Analytical Model to Replicate the Experimental Setup of Kikuchi et al.[17]

parameter	value
T	300 K
D	0.18 m^2/s
R	0.9 cm
L	30 cm
δ_P	761
δ_U	114

concentration was measured in experiments. δ_P represents the value of the similarity parameter with poisoned surface reactions, and δ_U represents the value with unpoisoned surface reactions.

Figure 6 shows the fraction of remaining H radicals down the length of the silica tube with poisoned and unpoisoned

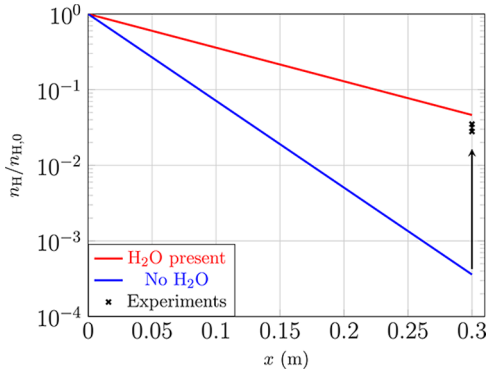

Figure 6. Fraction of remaining radicals down the centerline of the quartz tube (r = 0) with and without poisoning by water vapor. A radical source is located at x = 0. Here, a larger value means less recombination has occurred. Increase of $n_H(0.3)$ from expeiments is also shown.[17,31]

recombination coefficients, as predicted by the analytical model. As expected, the reduced recombination coefficient in the case with added water vapor results in a higher radical concentrations throughout the tube. As the distance from the radical source is increased, the disparity in radical concentration for the poisoned versus unpoisoned cases becomes more significant. At x = 30 cm, the fraction of remaining radicals is 122 times larger with water vapor than without it. In general, the hydrogen−water mixture needs over three times as much axial distance as the pure hydrogen gas to achieve the same level of radical destruction.

3.3. Comparison to Experiments. The poisoning effect of water on hydrogen recombination on silica has been observed

DOI: 10.1021/acs.jpcc.7b04675
J. Phys. Chem. C 2017, 121, 16366−16372

for a half-century.[13,19] However, the effect has been experimentally quantified only much more recently. Tomasini et al. used laser-induced stimulated emission (LISE) measurements of hydrogen density downstream of a hydrogen plasma indicated a room-temperature recombination coefficient on silica of $\gamma_H(300\ K) = 2.2 \times 10^{-3}$ for a pure H_2 feed gas.[32] Similar values have been obtained in past experiments.[13,33] This value is in close agreement with our model predictions of $\gamma_H(300\ K) = 3 \times 10^{-3}$ for unpoisoned recombination.

In LISE experiments, it was observed that the recombination coefficient dropped by an order of magnitude, down to $\gamma_H(300\ K) = 1.8 \times 10^{-4}$, when air was added to the feed gas (resulting in a 90% H_2, 10% air mixture). A similar drop is seen in our two-layer isotherm model when even a small amount of water vapor was added to the gas, with a recombination coefficient of $\gamma_H(300\ K) = 1 \times 10^{-4}$ for a mixture with 10% water. Experiments have shown that for small mixing ratios in the H_2 gas ($\leq$10% O_2) O_2 has a poisoning effect equal to that of water, while recombination rates are largely unchanged by the presence of N_2.[17,31] Thus, a comparable reduction in recombination coefficient is expected.

The poisoning effect of water has also been studied by directly measuring radical concentration down the length of a quartz tube, as in Figure 5.[17,31] In these experiments, the fraction of remaining hydrogen radicals at the end of a 30 cm tube was between 80 and 100 times larger for a feed gas of 1−80% water when compared to the fraction remaining in a pure H_2 feed gas. This range of experimental values has been added to Figure 6 by increasing our unpoisoned $n_H(x = 30\ cm)$ by factors of 80 and 100. This disparity in the fraction of remaining radicals is in quantitative agreement with the results of the analytical model in Section 3.2. When the poisoned recombination coefficient is used, the fraction of remaining radicals at $x = 30$ cm increases by a factor of 122. For the temperatures of these experiments, the single-layer isotherm model predicts no change in recombination activity when water vapor is added.

4. CONCLUSION

The poisoning of hydrogen recombination on silica by water adsorption is studied using a two-layer Langmuir isotherm model. In the two-layer model, hydrogen atoms chemisorb directly on the silica surface, while water molecules physisorb in a layer above the surface, blocking the adsorption and reaction of radical species. The two-layer model is suitable when chemisorption and physisorption sites are shared. If chemisorption and physisorption sites are distinct, the interaction of these two layers is reduced, and the single-layer model may adequately describe surface dynamics.

When water vapor is included in the hydrogen gas, the two-layer model predicts significantly lower recombination rates on the silica surface for temperatures below 400 K. At room temperature, the recombination coefficient of hydrogen on silica drops an order of magnitude—from $\gamma_H(300) = 3 \times 10^{-3}$ (pure H−H_2 gas) to $\gamma_H(300) = 1 \times 10^{-4}$ (hydrogen and water vapor). The poisoning effect in the two-layer model is insensitive to the water content of the gas mixture, consistent with experimental measurements which have found nearly uniform poisoning for water mixture ratios between 2% and 80%. The single-layer isotherm model predicts no poisoning of surface reactions for temperatures above 250 K.

An analytical solution is used to predict radical concentration in a semi-infinite tube with hydrogen recombination occurring at the walls. With water vapor, the reduced reactivity of the walls results in a higher radical concentration throughout the tube. The fraction of radicals remaining an axial distance of 30 cm from the radical source increases by 2 orders of magnitude when the recombination coefficient is switched from its unpoisoned to its poisoned value.

The predicted unpoisoned and poisoned values of the room-temperature recombination coefficient are in agreement with previous experiments with plasmas in pure hydrogen and hydrogen−air mixtures. The predicted rate of decay of radical concentration in the semi-infinite tube is also in agreement with experiments studying radical generation in hydrogen and hydrogen−water plasmas.

As shown in Figure 3, the two-layer model predicts a transition from poisoned to unpoisoned recombination at a temperature that is determined by the conditions in the gas phase. Experimental data are currently limited to poisoned and unpoisoned recombination coefficients at a fixed temperature. A better understanding of the poisoning behavior could be reached if the recombination coefficient was measured across a large temperature range for different mixture ratios of hydrogen and water (as was obtained by Kim and Boudart for the pure hydrogen case[11]).

The poisoning effect of water on heterogeneous hydrogen recombination has not been explored experimentally on oxide surfaces other than silica, though it appears the mechanisms of adsorption and reaction are similar. In general, water binds to hydroxyl groups on oxide surfaces with a relatively uniform heat of adsorption (14 kcal/mol on ceria[34] and 12.2 kcal/mol on titania[35]). Depending on the adsorption dynamics of hydrogen on these oxide surfaces, a similar poisoning effect may be observed. Competitive adsorption or reaction poisoning could pose serious problems for the performance of these materials in catalytic systems.

The poisoning effect of water on recombination appears to be unique to the hydrogen atom. Neither nitrogen nor oxygen recombination is hindered by the addition of water vapor to the mixture.[19] Atomic oxygen and nitrogen may not use surface hydroxyl groups as primary adsorption and reaction sites, resulting in the reduced influence of water on heterogeneous recombination rates of these species.

AUTHOR INFORMATION

Corresponding Author

*E-mail: htj@illinois.edu. Phone: (217) 265-5468.

ORCID

Kyle K. Mackay: 0000-0002-8978-2242

Notes

The authors declare no competing financial interest.

ACKNOWLEDGMENTS

This material is based in part upon work supported by the Department of Energy, National Nuclear Security Administration, under Award Number DE-NA0002374.

REFERENCES

(1) Lamb, R. N.; Furlong, D. N. Controlled Wettability of Quartz Surfaces. *J. Chem. Soc., Faraday Trans. 1* **1982**, *78*, 61−73.

(2) Hu, M.; Goicochea, J. V.; Michel, B.; Poulikakos, D. Water Nanoconfinement Induced Thermal Enhancement at Hydrophilic Quartz Interfaces. *Nano Lett.* **2009**, *10*, 279−285.

(3) Pashley, R.; Kitchener, J. Surface Forces in Adsorbed Multilayers of Water on Quartz. *J. Colloid Interface Sci.* **1979**, *71*, 491−500.

DOI: 10.1021/acs.jpcc.7b04675
J. Phys. Chem. C 2017, 121, 16366−16372

(4) Gurau, M. C.; Kim, G.; Lim, S.-M.; Albertorio, F.; Fleisher, H. C.; Cremer, P. S. Organization of Water Layers at Hydrophilic Interfaces. *ChemPhysChem* **2003**, *4*, 1231−1233.
(5) Aladdine, S.; Nygren, H. The Adsorption of Water and Amino Acids onto Hydrophilic and Hydrophobic Quartz Surfaces. *Colloids Surf., B* **1996**, *6*, 71−79.
(6) Bolis, V.; Fubini, B.; Marchese, L.; Martra, G.; Costa, D. Hydrophilic and Hydrophobic Sites on Dehydrated Crystalline and Amorphous Silicas. *J. Chem. Soc., Faraday Trans.* **1991**, *87*, 497−505.
(7) Smirnova, I.; Suttiruengwong, S.; Arlt, W. Feasibility Study of Hydrophilic and Hydrophobic Silica Aerogels as Drug Delivery Systems. *J. Non-Cryst. Solids* **2004**, *350*, 54−60.
(8) Jesionowski, T.; Krysztafkiewicz, A. Preparation of the Hydrophilic/Hydrophobic Silica Particles. *Colloids Surf., A* **2002**, *207*, 49−58.
(9) Bettens, B.; Verhoef, A.; van Veen, H. M.; Vandecasteele, C.; Degréve, J.; van der Bruggen, B. Adsorption of Pure Vapor Species on Microporous Silica Membranes and Silica Pellets. *J. Phys. Chem. C* **2010**, *114*, 9416−9423.
(10) Zhuravlev, L. The Surface Chemistry of Amorphous Silica. Zhuravlev Model. *Colloids Surf., A* **2000**, *173*, 1−38.
(11) Kim, Y. C.; Boudart, M. Recombination of Oxygen, Nitrogen, and Hydrogen Atoms on Silica: Kinetics and Mechanism. *Langmuir* **1991**, *7*, 2999−3005.
(12) Gelb, A.; Kim, S. K. Theory of Atomic Recombination on Surfaces. *J. Chem. Phys.* **1971**, *55*, 4935−4939.
(13) Wood, B. J.; Wise, H. The Kinetics of Hydrogen Atom Recombination on Pyrex Glass and Fused Quartz. *J. Phys. Chem.* **1962**, *66*, 1049−1053.
(14) Hickmott, T. Interaction of Atomic Hydrogen with Glass. *J. Appl. Phys.* **1960**, *31*, 128−136.
(15) St-Onge, L.; Moisan, M. Hydrogen Atom Yield in RF and Microwave Hydrogen Discharges. *Plasma Chem. Plasma Process.* **1994**, *14*, 87−116.
(16) Zyryanov, S.; Kovalev, A.; Lopaev, D.; Malykhin, E.; Rakhimov, A.; Rakhimova, T.; Koshelev, K.; Krivtsun, V. Loss of Hydrogen Atoms in H_2 Plasma on the Surfaces of Materials used in EUV Lithography. *Plasma Phys. Rep.* **2011**, *37*, 881−889.
(17) Kikuchi, J.; Suzuki, M.; Yano, H.; Fujimura, S. Effects of H_2O on Atomic Hydrogen Generation in Hydrogen Plasma. *Proc. SPIE* **1803**, *1993*, 70−76.
(18) Finch, G. Steam in the Ring Discharge. *Proc. Phys. Soc., London, Sect. A* **1949**, *62*, 465−482.
(19) Wise, H.; Wood, B. J. Reactive Collisions Between Gas and Surface Atoms. *Adv. At. Mol. Phys.* **1968**, *3*, 291−353.
(20) Rony, P. R.; Hanson, D. Effect of Oxygen, Nitrogen, and Water in Low-Pressure Hydrogen Discharges. *J. Chem. Phys.* **1966**, *44*, 2536−2538.
(21) Hackerman, N.; Hall, A. C. The Adsorption of Water Vapor on Quartz and Calcite. *J. Phys. Chem.* **1958**, *62*, 1212−1214.
(22) Whalen, J. Thermodynamic Properties of Water Adsorbed on Quartz. *J. Phys. Chem.* **1961**, *65*, 1676−1681.
(23) Mackay, K. K.; Freund, J. B.; Johnson, H. T. Hydrogen Recombination Rates on Silica from Atomic-Scale Calculations. *J. Phys. Chem. C* **2016**, *120*, 24137−24147.
(24) Fripiat, J.; Jelli, A.; Poncelet, G.; Andre, J. Thermodynamic Properties of Adsorbed Water Molecules and Electrical Conduction in Montmorillonites and Silicas. *J. Phys. Chem.* **1965**, *69*, 2185−2197.
(25) Taylor, D. E.; Runge, K.; Cory, M. G.; Burns, D. S.; Vasey, J. L.; Hearn, J. D.; Henley, M. V. Binding of Small Molecules to a Silica Surface: Comparing Experimental and Theoretical Results. *J. Phys. Chem. C* **2011**, *115*, 24734−24742.
(26) Masel, R. I. *Principles of Adsorption and Reaction on Solid Surfaces*; John Wiley & Sons: New York, 1996; Vol. 3.
(27) Kim, S. K. Temperature Dependence of the Rate of Termolecular Atomic Recombinations. *J. Chem. Phys.* **1967**, *46*, 123−127.
(28) Hirschfelder, J. O. Semi-Empirical Calculations of Activation Energies. *J. Chem. Phys.* **1941**, *9*, 645−653.
(29) Rajapakse, Y.; Wise, H. Diffusion and Heterogeneous Reaction. IX. Theoretical Analysis of Nonsteady-State Kinetics. *J. Chem. Phys.* **1968**, *48*, 3361−3364.
(30) Chapman, S.; Cowling, T. G. *The Mathematical Theory of Non-Uniform Gases: An Account of the Kinetic Theory of Viscosity, Thermal Conduction and Diffusion in Gases*; Cambridge university press: New York, 1970.
(31) Kikuchi, J.; Fujimura, S.; Suzuki, M.; Yano, H. Effects of H_2O on Atomic Hydrogen Generation in Hydrogen Plasma. *Jpn. J. Appl. Phys.* **1993**, *32*, 3120.
(32) Tomasini, L.; Rousseau, A.; Baravian, G.; Gousset, G.; Leprince, P. Laser Induced Stimulated Emission for Hydrogen Atom Density Measurements in a Hydrogen Pulsed Microwave Discharge. *Appl. Phys. Lett.* **1996**, *69*, 1553−1555.
(33) Sheen, D. B. Adsorption and Recombination of Hydrogen Atoms on Glass Surfaces. Part 1.−Method of Study and the Mechanism of Recombination at 77 and 273 K. *J. Chem. Soc., Faraday Trans. 1* **1979**, *75*, 2439−2453.
(34) Hayun, S.; Shvareva, T. Y.; Navrotsky, A. Nanoceria-Energetics of Surfaces, Interfaces and Water Adsorption. *J. Am. Ceram. Soc.* **2011**, *94*, 3992−3999.
(35) Raupp, G.; Dumesic, J. Adsorption of Carbon Monoxide, Carbon Dioxide, Hydrogen, and Water on Titania Surfaces with Different Oxidation States. *J. Phys. Chem.* **1985**, *89*, 5240−5246.

DOI: 10.1021/acs.jpcc.7b04675
J. Phys. Chem. C 2017, 121, 16366−16372